IMMPDAF Approach for Road Boundary Tracking

K. R. S. Kodagoda, S. S. Ge, *Fellow, IEEE,* W. S. Wijesoma, *Member, IEEE,* and A. P. Balasuriya, *Member, IEEE*

***Abstract*— Robust road boundary extraction/tracking is one of the main problems in autonomous roadway navigation. Though the road boundary can be defined by various means including lane markings, curbs and borders of vegetation, this paper focuses on road boundary tracking using curbs. A vehicle mounted (downward tilted) two-dimensional (2D) laser measurement system (LMS) is utilized to detect the curbs. The tracking problem is difficult because both the vehicle is moving, and the target is disappearing, reappearing and maneuvering in clutter. The Interacting Multiple Model Probabilistic Data Association Filter (IMMPDAF) is proposed to solve the problems after detailed analysis. Track initiation, confirmation and deletion are performed using Sequential Probability Ratio Test (SPRT). Extensive simulations followed by experiments in a campus environment show that the road boundary tracking utilizing curbs is possible and robust through IMMPDAF.**

***Index Terms*— Laser radar, road transportation, robot sensing systems, autonomous vehicles.**

I. Introduction

ROAD safety is a worldwide concern and has yet to be solved satisfactorily [1]. Sensing, detection and tracking of roads are essential in intelligent and safe operation. Different technologies have been investigated for road boundary detection and tracking including, camera [2-4], millimeter wave radar (MMWR) [5-6] and laser measurement systems (LMSs) [7-8]. Camera based methods are the most extensively researched and tested as it has the advantages of high information content, low costs, low operating power and absence of a sweep time. But, it performs poorly in bad illumination. Though MMWR has the ability to provide good quality image of a road scene ahead over longer distances (1m-200m) in snow, haze, dust, rain, and is not susceptible to ambient light, it is still very expensive. The utilization of LMSs in automotive applications is on the rise due to their low cost and operating power, and small sizes as compared with MMWR. In this work, we utilize an LMS for detection of curbs and hence road boundaries.

The complex curb tracking can be considered as tracking of a maneuvering target in clutter. Adaptive techniques are usually used for the state estimation of maneuvering targets. Multiple model approach, such as the Interacting Multiple Model (IMM) [15], provides one of the most effective frameworks for tracking maneuvering targets [13]. Cluttered data complicate the maneuver detection and data association, which can be effectively handled in the framework of the Probabilistic Data Association (PDA) [15]. The integration of IMM with PDA is collectively called IMMPDAF in the literature [15]. IMMPDAF has been applied to target tracking with radar sensors [15, 20], passive sensors, such as infrared cameras [19], and multi-sensory systems (radar and an infrared sensor) in clutter [18, 22]. In this work, we make an attempt to apply the IMMPDAF for curb tracking using a laser measuring system, which can be effectively incorporated into motion planning [9-10] and localization [11] in practice. The effectiveness of the proposed problem formulation and solution is demonstrated through extensive simulations and comparison with IMM and nearest neighbor data association, followed by realistic and thorough experimentations on a full size, car-like mobile robot in actual road environments.

The main contributions of the paper are as follows: (i) A novel method is presented in formulating the curb tracking problem (using an LMS) as tracking a maneuvering line target in clutter with a moving observer, which successfully overcomes the inherent problems of curb tracking caused by conflicts between maneuver detection and data association; (ii) The problems of disappearances and reappearances of the curbs (e.g. in intersections) are conveniently solved by geometric road constraints coupled with a probabilistically determined track termination and track initialization; and (iii) Problems due to irregularities of road surface, water puddles or objects on the road are minimized by devising a methodology to detect/track vertical curb surfaces.

In Section II, the problem of road boundary tracking is formulated. The IMMPDAF algorithm is described in Section III. In Section IV, simulations and experimental results are presented for various road scenarios. Section V concludes the paper giving future directions.

Manuscript received December 2, 2003.

K. R. S. Kodagoda was with the National University of Singapore. He is now with the ARC Centre of Excellence for Autonomous Systems, Australia. (e-mail: s.kodagoda@cas.edu.au)

S. S. Ge is with the Department of Electrical and Computer Engineering, National University of Singapore. (e-mail: elegesz@nus.edu.sg, phone (+65) 6874 6821, fax. (+65) 6779 1103)

W. S. Wijesoma is with the school of EEE, Nanyang Technological University, Singapore (e-mail: eswwijesoma@ntu.edu.sg).

A. P. Balasuriya is with MIT, USA (arjunab@mit.edu).

II. Problem Formulation

The main objective of this work is to extract and track road boundaries in urban and semi-urban environments. Such environments inherently consist of curbs defining the road boundaries. In this work, it is perceived that the road boundaries are defined by the temporal evolution of line segments corresponding to the vertical surfaces of curbs, which can be extracted by a looking down (α_L =2.6^o), front mounted 2D LMS as shown in Fig. 1. When the vehicle is in motion (moving observer) the line segments or targets move along the curbs (left/right). Straight road ahead defines a non-maneuvering target state. Road bend ahead defines a maneuvering target state. The curb tracking problem becomes nontrivial due to the maneuvering nature, vanishing and reappearance of the target and the presence of clutter. It is further complicated by the utilization of a moving observer. IMMPDAF offers one of the most effective and robust techniques to handle such targets with modest computational requirements [15].

A. Process Model

The moving observer or the car-like vehicle process model can be derived from Fig. 2 as:

$$\mathbf{s}^v(k+1)=\begin{bmatrix} x_w^v(k)+\Delta T V(k)\cos\phi_w^v(k) \\ y_w^v(k)+\Delta T V(k)\sin\phi_w^v(k) \\ \phi_w^v(k)+\dfrac{\Delta T V(k)\tan\gamma(k)}{L}\end{bmatrix}+\mathbf{v}^v(k+1) \quad (1)$$

where the states are given by $\mathbf{s}^v=\begin{bmatrix} x_w^v & y_w^v & \phi_w^v\end{bmatrix}^T$, $\{x_w^v, y_w^v\}$ are the coordinates of the center of the rear axel of the vehicle, ϕ_w^v is the orientation of the vehicle axis with respect to the world coordinate system shown in Fig. 2, V and ΔT are the speed of the vehicle and sampling time respectively, γ and L are steer angle and wheel base length respectively, and $\mathbf{v}^v(k+1)$ is the zero mean Gaussian process noise.

In this tracking problem, the target (i.e., the curb) is represented as a line segment denoted by the mid point (x,y) and orientation, ϕ. For the left-bend and right-bend curb scenarios (equivalent to a maneuvering target), the usual turn rate model in world coordinate system is utilized [14]:

$$\mathbf{s}^t(k+1)=\begin{bmatrix} x_w^c(k)+\bar{m}\dot{x}_w^c(k)-\bar{n}\dot{y}_w^c(k) \\ (1-\bar{n}\omega)\dot{x}_w^c(k)-\bar{m}\omega\dot{y}_w^c(k) \\ y_w^c(k)+\bar{m}\dot{y}_w^c(k)+\bar{n}\dot{x}_w^c(k) \\ (1-\bar{n}\omega)\dot{y}_w^c(k)+\bar{m}\omega\dot{x}_w^c(k) \\ \omega\Delta T+\phi_w^c(k)\end{bmatrix}+\begin{bmatrix} 0.5\Delta T^2 & 0 \\ \Delta T & 0 \\ 0 & 0.5\Delta T^2 \\ 0 & \Delta T \\ 0 & 0\end{bmatrix}\mathbf{v}^t(k+1)$$

$$\bar{m}=\frac{\sin\omega\Delta T}{\omega},\ \bar{n}=\frac{(1-\cos\omega\Delta T)}{\omega} \quad (2)$$

where the states are $\mathbf{s}^t=\begin{bmatrix} x_w^c & \dot{x}_w^c & y_w^c & \dot{y}_w^c & \phi_w^c\end{bmatrix}^T$, $\{x_w^c, y_w^c\}$ are the coordinates of the mid point of the line segment (target) corresponding to a curb, ϕ_w^c is the orientation of the line segment, $\{\dot{x}_w^c, \dot{y}_w^c\}$ are the target's speeds along the *x* and *y* axes, $\mathbf{v}^t(k+1)$ is the process noise (zero mean Gaussian), ω is the turn rate of the target and can be assigned a few values to define several models including $\omega=0$ for constant velocity model (for straight curb scenario).

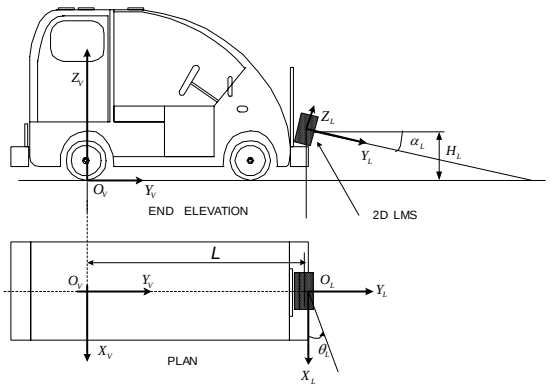

Fig.1. Sensor mounting and coordinate systems

Suppose that $\{M(k+1)\}$, $k\geq 0$ represents the target operational regime or mode at time *k+1* and assume that *M* evolves as a homogeneous, discrete-time Markov process in the state space $\{1,....,r\}$ with transition probability matrix $\mathbf{T}_{ij}=P(M(k+1)=j\,|\,M(k)=i)$ with initial conditions, $P(M(0)=i)=\boldsymbol{\pi}_0(i)$. Then, the composite nonlinear vehicle and target dynamics (1) - (2) can be described as:

$$\begin{aligned}\mathbf{s}(k+1)&=\begin{bmatrix}\mathbf{s}^v(k+1)^T & \mathbf{s}^t(k+1)^T\end{bmatrix}^T \\ &=\mathbf{f}\left[M(k+1),\mathbf{s}(k)\right]+\mathbf{B}(M(k+1))\mathbf{v}(k+1)\end{aligned} \quad (3)$$

where $\mathbf{s}(k),\mathbf{v}(k)\in\mathbb{R}^n$ with $\mathbf{s}(0)$ a Gaussian random vector, $\mathbf{f}\left[M(k+1),\mathbf{s}(k)\right]$ is the mode dependant nonlinear state transition matrix, and $\mathbf{B}(M(k+1))$ is the mode dependent matrix defined by (1) and (2), The process noise, $\mathbf{v}(k+1)$ is a sequence of independent zero mean Gaussian random vectors with positive definite covariance matrix, $\mathbf{Q}$. The process noise, $\mathbf{v}(k+1)$ and $\mathbf{s}(0)$ are uncorrelated.

As depicted in Fig. 2, the road curb (line) segment in world coordinates is represented by $\{x_w^c, y_w^c, \phi_w^c\}$, and the observation model:

$$\begin{bmatrix} x_w^{gps}(k+1) \\ y_w^{gps}(k+1) \\ \phi_w^{gyro}(k+1) \\ x_L^c(k+1) \\ y_L^c(k+1) \\ \phi_L^c(k+1)\end{bmatrix}^T=\begin{bmatrix} x_w^v(k+1) \\ y_w^v(k+1) \\ \phi_w^v(k+1) \\ \bar{a}\cos\phi_w^v(k+1)+\bar{b}\sin\phi_w^v(k+1)-a \\ -\bar{a}\sin\phi_w^v(k+1)+\bar{b}\cos\phi_w^v(k+1)-b \\ \pi/2+\phi_w^c(k+1)-\phi_w^v(k+1)\end{bmatrix}+\mathbf{w}(k+1) \quad (4)$$

where, $\bar{a} = x_w^c(k+1) - x_w^v(k+1)$, $\bar{b} = y_w^c(k+1) - y_w^v(k+1)$, $x_w^{gps}, y_w^{gps}, \phi_w^{gyro}$ are the measurements of vehicle position (using global positioning system, GPS) along *x*-axis, *y*-axis and vehicle orientation measured using a gyroscope respectively. $\{x_L^c, y_L^c, \phi_L^c\}$ is the curb data extracted by the laser scanner in laser coordinate system, and constants *a* and *b* are as defined in Fig. 2.

Therefore, the measurement model of the hybrid vehicle and LMS sensor is,

$$\mathbf{z}(k+1) = \mathbf{h}\left[\mathbf{s}(k+1)\right] + \mathbf{w}(k+1) \tag{5}$$

where, $\mathbf{z}(k) = [x_w^{gps}(k+1), y_w^{gps}(k+1), \phi_w^{gyro}(k+1), x_L^c(k+1), \ldots$ $y_L^c(k+1), \phi_L^c(k+1)]^T$, $\mathbf{w}(k) \in \mathbb{R}^m$ a sequence of zero mean Gaussian random vectors with covariance matrix $\mathbf{R}$; the process $\mathbf{v}(k)$ is uncorrelated with $\mathbf{w}(k)$, $\mathbf{s}(0)$ and $\{M(k)\}$.

The aim is now to find the hybrid vehicle and target state estimate, $\mathbf{s}(k+1)$, given the measurements, $\mathbf{Z}(k+1) = \{\mathbf{z}(1), \ldots, \mathbf{z}(k+1)\}$.

III. IMMPDAF Algorithm

Curb tracking can be formulated as a problem of tracking a maneuvering target in clutter. This section describes the utilization of IMMPDAF to solve for it.

A. Track Formation and Termination

False track initiations give rise to missed detections, which may lead to track loss. Therefore, track initiation is an important aspect of the tracking algorithm, and in this paper, it is handled in the manner described as follows.

An unscented Kalman filter (UKF) [21] based approach is used for laser data segmentation and line parameter estimation [12]. Each segment is then analyzed through a sequence of filtering [12] to obtain the line segments corresponding to the road curbs. The midpoint of a line segment, $\{x_L, y_L\}$ is estimated as the mean of LMS data (in Cartesian coordinates) in a particular segmented data set, and ϕ_L is directly estimated through UKF.

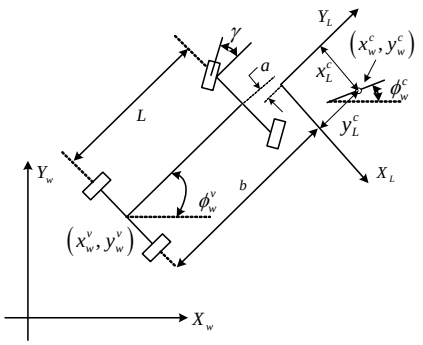

Fig. 2. Vehicle kinematics

Although the initial tracks determined through the above procedure are robust to various road scenarios, there can be a little possibility that those are due to clutter. Therefore, these initial tracks are used to form tentative tracks and ideas from the integrated probabilistic data association (IPDA) [16] with SPRT [13] are used for track confirmation and termination. Using the Markov relationship, the probability of existence of the true target, $P_T(k+1|k)$ before the receipt of data in scan *k+1* is [17],

$$P_T(k+1|k) = P_{22}P_T(k|k) + P_{12}\left[1 - P_T(k|k)\right] \tag{6}$$

where P_{22} is the probability of transition from observable state to observable state, whilst P_{12} is the probability of transition from unobservable state to observable state. Then, the update of the probability of target existence is [16],

$$P_T(k+1|k+1) = \frac{1-\delta_{k+1}}{1-\delta_{k+1}P_T(k+1|k)} P_T(k+1|k) \tag{7}$$

where δ_{k+1} is defined as

$$\delta_{k+1} = \begin{cases} P_D P_G & N_{k+1} = 0 \\ P_D P_G \left[1 - \overline{V} \sum_{i=1}^{N_{k+1}} \frac{1}{P_G (2\pi)^{M/2} \sqrt{|S(k+1)|}} e^{-d_i^2/2} \right] & \text{Otherwise} \end{cases}$$

$\overline{V} = \frac{V_{G_{k+1}}}{\left(N_{k+1} - P_D P_G P_T(k+1|k)\right)}$, P_D is the probability of detection, P_G is the gate probability, V_G is the gate volume, N_{k+1} is the number of measurements inside the validation gate, S is the innovation covariance, and d_i^2 is the normalized innovation squared of the i^{th} measurement.

The Log Likelihood Ratio, LLR, can now be defined as [13],

$$LLR_{k+1} = \ln\left(\frac{P_T}{1-P_T}\right) \tag{8}$$

Once the LLR is obtained, track confirmation and termination thresholds are determined using the SPRT [13] as,

$$LLR_{k+1} \geq \ln\left(\frac{1-\beta_T}{\alpha_T}\right), \text{ declare track confirmation}$$

$$\ln\left(\frac{\beta_T}{1-\alpha_T}\right) < LLR_{k+1} < \ln\left(\frac{1-\beta_T}{\alpha_T}\right), \text{ continue test}$$

$$LLR_{k+1} \leq \ln\left(\frac{\beta_T}{1-\alpha_T}\right), \text{ delete track}$$

where, α_T is the probability of false track confirmation, and β_T is the probability of true track termination.

B. Track Maintenance

The IMMPDAF is capable of tracking highly maneuvering targets [15]. Therefore, it is used for track maintenance as

detailed below.

1. Mixing probabilities: In the IMM algorithm, input to the filter matched to the model *j* is computed using estimates with probabilistic weightings called *mixing probabilities*, and are calculated as,

$$\mu_{ij}(k) = P\{M_i(k) \mid M_j(k+1), \mathbf{Z}^k\} = \frac{1}{\bar{c}_j}\mathbf{T}_{ij}\mu_i(k) \tag{9}$$

where $\mu_{ij}(k)$ is the conditional probability that the target transitioned from state *i* to state *j* at scan *k*, $\mu_i(k)$ is the probability that the target is in mode *i* as computed just after data are received on scan *k*, $\mathbf{T}_{ij}$ is the mode transition probability matrix, and $\bar{c}_j$ is the normalization constant, which is defined by, $\bar{c}_j = \sum_{i=1}^{r}\mathbf{T}_{ij}\mu_i(k)$.

2. Mixing: Starting with $\hat{\mathbf{s}}^i(k \mid k)$, the mixed initial conditions for the filter matched to mode, $M_j(k+1)$ can be computed as,

$$\hat{\mathbf{s}}^{oj}(k \mid k) = \sum_{i=1}^{r}\hat{\mathbf{s}}^i(k \mid k)\mu_{ij}(k) \tag{10}$$

$$\hat{\mathbf{P}}^{oj}(k \mid k) = \sum_{i=1}^{r}\mu_{ij}(k)\left\{\hat{\mathbf{P}}^j(k \mid k) + \bar{\tilde{\mathbf{s}}}(k \mid k)\bar{\tilde{\mathbf{s}}}^T(k \mid k)\right\} \tag{11}$$

where $\bar{\tilde{\mathbf{s}}}(k \mid k) = \hat{\mathbf{s}}^i(k \mid k) - \hat{\mathbf{s}}^{oj}(k \mid k)$

3. State prediction and associated covariance: With the nonlinear process model, state prediction and covariance calculation are carried out using the standard extended Kalman filter (EKF).

$$\bar{\mathbf{s}}^j(k+1) = \mathbf{f}\left(\hat{\mathbf{s}}^{oj}(k \mid k), M_j(k+1)\right) \tag{12}$$

$$\bar{\mathbf{P}}^j(k+1) = \mathbf{F}^j\hat{\mathbf{P}}^{oj}(k \mid k)\mathbf{F}^{jT} + \mathbf{B}^j\mathbf{Q}\mathbf{B}^{jT} \tag{13}$$

where $\mathbf{F}^j = \left.\frac{\partial \mathbf{f}}{\partial \mathbf{s}}\right|_{\mathbf{s}=\hat{\mathbf{s}}^j(k|k)}$.

4. Measurement prediction and validation: Since the measurement model is nonlinear, EKF based linearization is performed and used in the covariance calculation.

$$\hat{\mathbf{z}}^j(k+1) = \mathbf{h}\left[\bar{\mathbf{s}}^j(k+1)\right] \tag{14}$$

$$\mathbf{S}^j(k+1) = \mathbf{H}^j\bar{\mathbf{P}}^j(k+1)\mathbf{H}^{jT} + \mathbf{R} \tag{15}$$

where $\mathbf{H}^j = \left.\frac{\partial \mathbf{h}}{\partial \mathbf{s}}\right|_{\mathbf{s}=\hat{\mathbf{s}}^j(k+1|k)}$.

The measurements, $\mathbf{z}_l^j(k+1);\ l = 1,...,N_{k+1}$, are validated if and only if, $\left[\mathbf{z}_l^j(k+1) - \hat{\mathbf{z}}^j(k+1)\right]\mathbf{S}^j(k+1)^{-1}\left[\mathbf{z}_l^j(k+1) - \hat{\mathbf{z}}^j(k+1)\right]^T \le \gamma_G$ where, $\left[\mathbf{z}_l^j(k+1) - \hat{\mathbf{z}}^j(k+1)\right]$ is the measurement residual of the j^{th} mode, $\mathbf{S}^j(k+1)$ is the innovation covariance of the j^{th} mode, and γ_G is the threshold, which is determined using chi-square tables.

5. Likelihood calculation and mode probability update: The likelihood function Λ^j is calculated for each mode *j*. This includes N_{k+1} data association hypotheses corresponding to each observation ($l = 1,.....,N_{k+1}$) in the gate and the hypothesis that none of the observation is valid.

$$\Lambda^j(k+1) = (1 - P_D P_G)\beta_D + \sum_{l=1}^{N_{k+1}}\frac{P_D e^{-d_{lj}^2/2}}{\sqrt{(2\pi)^M\left|\mathbf{S}^j(k+1)\right|}} \tag{16}$$

where $\beta_D = N_{k+1}/V_G$, and d_{lj}^2 is the square of the Mahalanobis distance associated with the predicted measurement of the j^{th} mode with l^{th} measurement within the gate. Then, the mode probabilities are updated as

$$\bar{\mu}_j(k+1) = \Lambda^j(k+1)\mu_j(k)/c, \quad c = \sum_{j=1}^{r}\Lambda^j(k+1)\mu_j(k) \tag{17}$$

6. State and covariance update using nonparametric version of PDA [18]: The probabilities associated with $N_{k+1}+1$ hypotheses that assign observation *i* to track *j* are computed through,

$$p_{ji} = \begin{cases} \dfrac{b^*}{b^* + \sum_{l=1}^{N_{k+1}}\alpha_{jl}}, & i = 0 \\ \dfrac{\alpha_{ji}}{b^* + \sum_{l=1}^{N_{k+1}}\alpha_{jl}}, & i = 1,..,N_{k+1} \end{cases} \tag{18}$$

where $b^* = (1 - P_D P_G)\beta(2\pi)^{M/2}\sqrt{\left|\mathbf{S}^i\right|}$, and $\alpha_{ij} = P_D e^{-d_{ij}^2/2}$.

Then, the standard EKF state update is,

$$\begin{aligned} \hat{\mathbf{s}}^j(k+1 \mid k+1) &= \hat{\mathbf{s}}^j(k+1 \mid k) + \mathbf{K}(k+1)\mathbf{v}_j(k+1) \\ \mathbf{v}_j(k+1) &= \sum_{l=1}^{N_{k+1}} p_{jl}\left(\mathbf{z}^l(k+1) - \hat{\mathbf{z}}^j(k+1)\right) \\ \mathbf{K}(k+1) &= \bar{\mathbf{P}}^j(k+1)\mathbf{H}^{jT}\mathbf{S}^j(k+1)^{-1} \end{aligned} \tag{19}$$

The covariance has to be updated considering the uncertainties associated with the PDA. Therefore, it can be computed as:

$$\begin{aligned} \hat{\mathbf{P}}^j(k+1 \mid k+1) &= \mathbf{P}^0(k+1 \mid k+1) + d\mathbf{P}(k+1) \\ \mathbf{P}^0(k+1 \mid k+1) &= p_{i0}\bar{\mathbf{P}}^j(k+1) + (1 - p_{i0})\mathbf{P}^*(k+1 \mid k+1) \\ \mathbf{P}^*(k+1 \mid k+1) &= \left[\mathbf{I} - \mathbf{K}(k+1)\mathbf{H}^j\right]\bar{\mathbf{P}}^j(k+1) \\ d\mathbf{P}(k+1) &= \mathbf{K}(k+1)\left[\sum_{l=1}^{N_{k+1}}\left(p_{jl}\mathbf{v}_{jl}\mathbf{v}_{jl}^T\right) - \mathbf{v}_j\mathbf{v}_j^T\right]\mathbf{K}(k+1)^T \end{aligned} \tag{20}$$

where $\mathbf{P}^0(k+1|k+1)$ is the covariance calculated assuming a single correct measurement association, and $d\mathbf{P}(k+1)$ is the incremental term added to compensate for the uncertainty in data association.

7. Output step: Combination of the model conditioned states and covariances are performed for output purposes. Note that these are not parts of the recursive filter.

$$\tilde{\mathbf{s}}(k+1|k+1) = \sum_{j=1}^{r} \hat{\mathbf{s}}^j(k+1|k+1)\bar{\mu}_j(k+1)$$
$$\tilde{\mathbf{P}}(k+1|k+1) = \sum_{j=1}^{r} \bar{\mu}_j(k+1)\left\{\hat{\mathbf{P}}^j(k+1|k+1) + \tilde{\tilde{\mathbf{s}}}.\tilde{\tilde{\mathbf{s}}}^T\right\} \quad (21)$$

where $\tilde{\tilde{\mathbf{s}}} = \hat{\mathbf{s}}^j(k+1|k+1) - \tilde{\mathbf{s}}(k+1|k+1)$.

IV. Simulation and Experimental Results

A. Simulation Results

A simulation study[1] has been carried out to compare the performance of the IMM Global Nearest Neighbor Filter (IMMGNNF) with IMMPDAF and to analyze the robustness of the IMMPDAF in the road boundary tracking application. The sensors used are the vehicle mounted 2D LMS, GPS and gyroscope. The LMS is assumed to be capable of detecting line segments with measurement errors of $\sigma_{x_L} = 0.1m$, $\sigma_{y_L} = 0.1m$, $\sigma_{\phi_L} = 0.01rad$ .The vehicle pose measurement errors are assumed to be $\sigma_{x_v} = 0.1m, \sigma_{y_v} = 0.1m, \sigma_{\phi_v} = 0.01rad$. All the sensor-errors are assumed to be zero mean Gaussian distributions.

The vehicle is assumed to be traveling at a speed of 3ms^{-1} along the trajectory, A-F, as shown in Figs. 3 and 4. The route consists of straight portions and bends with or without observations. The clutter is Poisson distributed with density 2.9x10^{-4}. Segment B-C resembles a cross road, where there are no curbs present on both sides of the road. Segment D-E resembles a right road branching at a bend, where there is no curb on the right side of the road. Three modes are considered: *Mode 1* refers to straight road ahead ((2) with $\omega = 0$), *Mode 2* refers to left turns ((2) with $\omega = 0.3$ rad/s) and *Mode 3* refers to right turns ((2) with $\omega = -0.3$ rad/s). The mode transition probability matrix used for the simulation is,

$\mathbf{T} = \begin{pmatrix} 0.8 & 0.1 & 0.1 \\ 0.1 & 0.8 & 0.1 \\ 0.1 & 0.1 & 0.8 \end{pmatrix}$. The diagonal elements show that the target is more probable to be in the same mode. It can practically be achieved through the utilization of higher sampling rates.

The position tracking performance of IMMPDAF is shown in Fig. 5 (a), while the orientation tracking performance is shown in Fig. 5 (b). It is interesting to consider the segment B-C and D-E, where there are no curbs present. The expanded B-C and D-E segments with uncertainty ellipses of the estimated vehicle and curb positions are shown in Fig. 5 (c) and (d). During these periods, the IMM simply predicts without updating. It can be noted in Fig. 5 (e), the log likelihood ratios, LLRs, of both right hand side and left hand side curbs start to decrease after reaching position 'B' performing track termination. Although the tracks are being terminated (LLR bellow T1), the IMM simply predicts the states until there are observations fall with in the validation gate. Once it finds an observation, a tentative track is initiated and a LLR is calculated for the confirmation as seen from position 'C' of Fig. 5 (e). Once the LLR exceeds the threshold, T2, the track is confirmed as originated from a true target. A similar explanation can be given for the segment D-E, however, with only right hand track is being terminated whilst the left hand track is a confirmed track. Fig. 5 (f) and (g) show the mode probabilities calculated in the IMMPDAF, which correctly resembles each road segment.

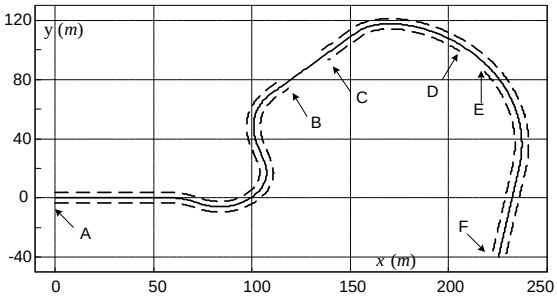

Fig. 3. Vehicle path and curbs: vehicle path – *solid line*, curbs – *dashed lines*

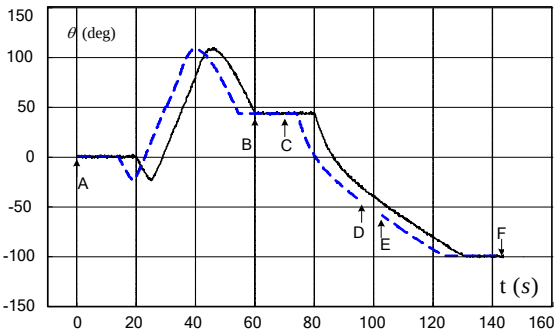

Fig. 4 Orientations: vehicle yaw – *solid*, curb orientation – *dashed*

Fig. 6 (a) and (b) show the root mean square (RMS) position errors in x-direction, Fig. 7 (a) and (b) show the RMS position error in y-direction and Fig. 8 (a) and (b) show the RMS orientation error for 50 Monte Carlo runs of the IMMPDAF and IMMGNNF. In all Figures, the IMMPDAF has a smaller RMS error when comparing with IMMGNNF. This shows that the tracking performance of a maneuvering target in clutter can be improved by utilizing all the observations in the validation gate when comparing with the most probable single observation, such as in IMMGNNF.

[1]It should be noted that the process model for a maneuvering target is not known and it is achieved as a probabilistically weighted outputs of a few number of target models, and utilizes a bank of extended Kalman filters. Furthermore, the track initialization and termination are also handled within the filter. This makes the theoretical performance analysis of the IMMPDAF extremely hard, and thus these analyses are commonly performed based on simulation experiments.

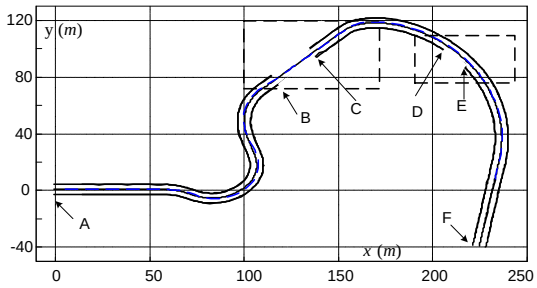

(a) IMMPDAF position tracking results: actual curbs and vehicle positions – *dashed*, IMMPDAF estimated positions – *solid*.

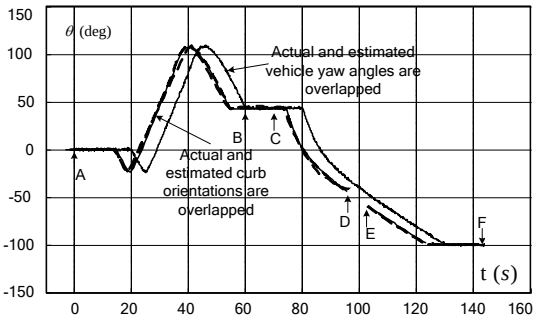

(b) IMMPDAF orientation tracking results: actual curbs and vehicle orientations – *dashed*, IMMPDAF estimated orientations – *solid*.

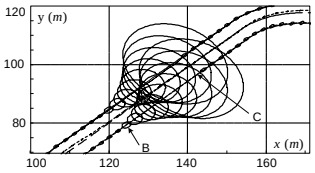

(c) Expanded B-C segment with uncertainty ellipses of vehicle and curb positions: actual positions – *dashed*, predicted positions – *dotted*

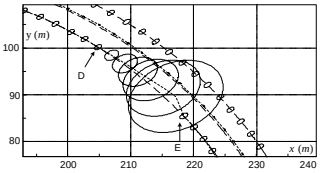

(d) Expanded D-E segment with uncertainty ellipses of vehicle and curb positions: actual positions – *dashed*, predicted positions – *dotted*

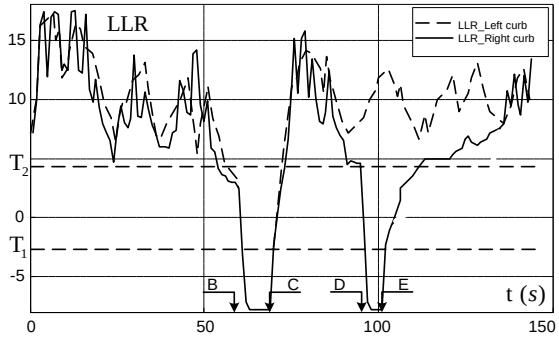

(e) LLRs of right hand and left hand side curbs

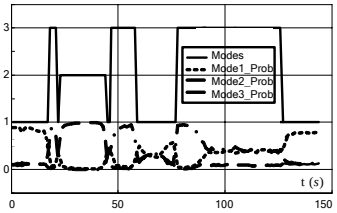

(f) Mode probabilities refer to the left hand side curb

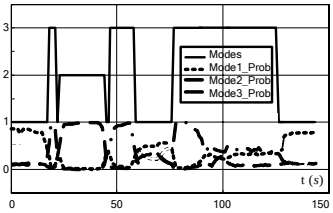

(g) Mode probabilities refer to the right hand side curb

Fig. 5. IMMPADF tracking performance

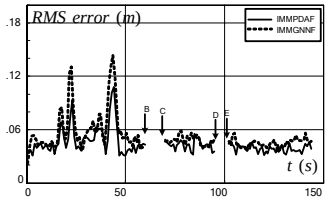

(a) Right hand side curb

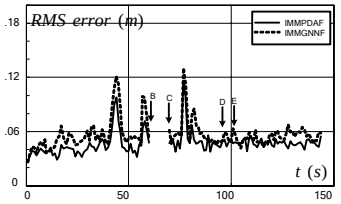

(b) Left hand side curb

Fig. 6 Position RMS error in x- direction for 50 runs

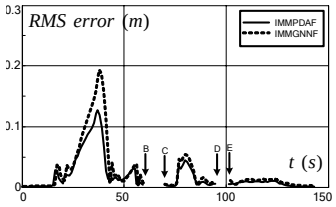

(a) Right hand side curb

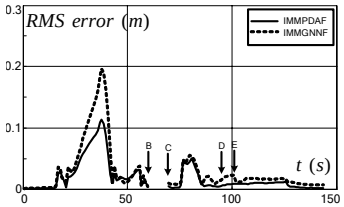

(b) Left hand side curb

Fig. 7 Position RMS error in y- direction for 50 runs

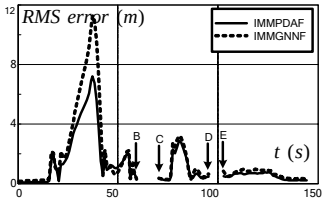

(a) Right hand side curb

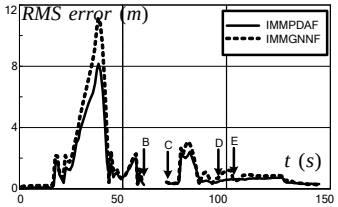

(b) Left hand side curb

Fig. 8 RMS error in orientation for 50 runs

B. Experimental Results

The robustness of the IMMPDAF algorithm for curb tracking was evaluated experimentally using a car-like vehicle [12] equipped with onboard computers, a looking down 2D LMS, four wheel encoders, one steering wheel encoder, a GPS and a gyroscope. The speed (V in (1)) and steering angle (γ in (1)) were determined by the wheel and steering encoders respectively, and were known quantities. The sampling time was 100ms. The vehicle was driven at a speed of 4ms^{-1} at a hilly test site, which had straight road segments, bend, right road branching and a x-intersection.

Fig. 9 shows the curb tracking results using the IMMPDAF in various road scenarios including straight road segments, bend, right road branching and x-intersection. Fig. 10 (a) shows consecutive laser data corresponding to the window, *W1*, in Fig. 9 (a), which is a straight road segment. In the plot, data in between y = 4m and y = -4m correspond to the road surface and curbs. On the left side of the road is a bank, and scatter data on the right hand side is due to trees, poles and other man-made structures. The data corresponding to the road surface forms a "V" shape due to the cylindrical nature of the road surface.

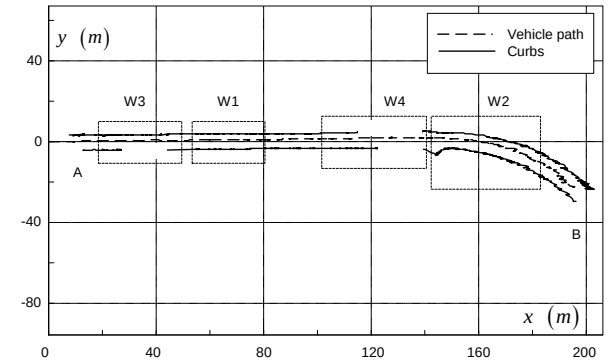

(a) Position tracking

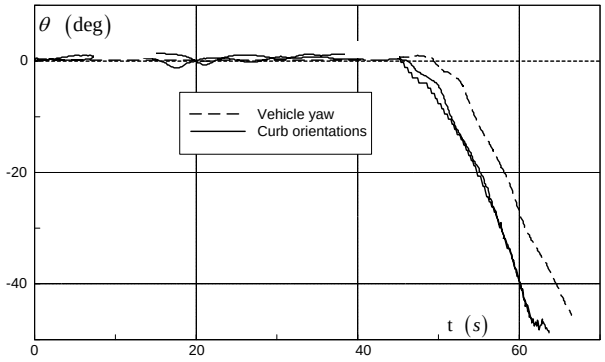

(b) Orientation tracking

Fig. 9 Experimental curb tracking results using IMMPDAF

Figure 10 (b) shows the laser data corresponding to the window, *W2*, of Fig. 9 (a), which is a right turn. Window, *W3*, in Fig. 9 (a) corresponds to a right road branching and laser data is shown in Fig. 10 (c). In this portion of the road, the right hand side track is terminated (see Fig. 9) due low LLR. Then, the IMMPDAF simply predicts the states until a new observation is available. Once it receives an observation, it goes through a series of filters namely, the orientation filter, neighborhood filter and road width filter [12] before a tentative track is initiated. Then, SPRT is carried out for track confirmation. Fig. 10 (d) shows the laser data referring to the window, *W4*, in Fig. 9 (a). It corresponds to an x- intersection where there are no curbs present on both sides of the road. As seen from Fig. 9, both tracks are being deleted during the x-intersection and both were reinitiated after the x-intersection showing the robustness to target loss and reappearing.

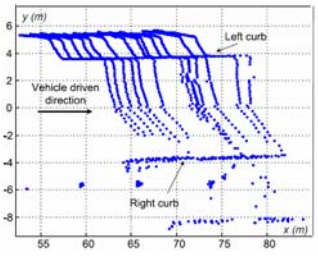

(a) Laser data corresponding to *W1* of Fig. 9 (a)

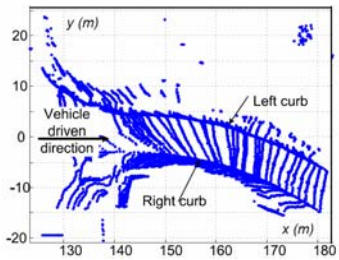

(b) Laser data corresponding to *W2* in Fig. 9 (a)

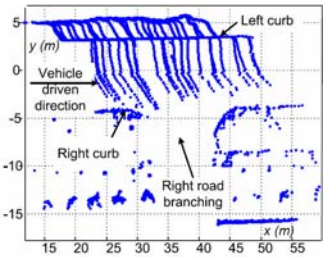

(c) Laser data corresponding to *W3* in Fig. 9 (a)

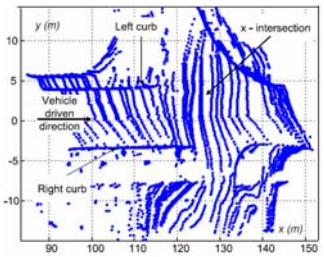

(d) Laser data corresponding to *W4* in Fig. 9 (a)

Fig. 10. Laser data corresponding to windows, *W1*, *W2*, *W3* and *W4*.

V. Conclusion

In this paper, we have proposed a method of extracting and tracking of road boundaries using curbs. The tracking problem becomes nontrivial due to the utilization of a moving observer (vehicle), presence of clutter, and maneuvering nature of the target with disappearances and reappearances. The tracking problem has been successfully solved with an IMMPDAF framework. Track initiation, confirmation and deletion were handled using SPRT. Extensive simulation studies showed that the IMMPDAF is superior to that of IMMGNNF. The experimental results on a campus environment showed that the proposed methodology is robust in all the tested road scenarios including, straight segments, bends, loss and reappearing of curbs due to road branching and x-intersections. Temporary obstruction of curbs by passing vehicles can be successfully handled as in road branching or x-intersections. It can be concluded that the road boundary tracking via curb tracking is viable and effective.

References

[1] R. Lamm, B. Psarianos, and T. Mailaender, *Highway Design and Traffic Safety Engineering Handbook*, Newyork, McGraw-Hill, 1999.

[2] D. Pomerleau and T. Jochem, "Rapidly adapting machine vision for autonomated vehicle steering", *IEEE Expert*, Vol.11, Issue: 2 , pp.19 – 27, April 1996.

[3] E. D. Dickmanns and B. D. Mysliwetz, "Recursive 3D road and relative ego-state recognition", *IEEE Trans. Pattern Anal. and Machine Intell.*, Vol.14, No.2, pp.199-213, Feb. 1992.

[4] M. Bertozzi and A. Broggi, "GOLD: A parallel real-time stereo vision system for generic obstacle and lane detection", *IEEE Trans. Image Processing*, Vol.7, No.1, pp.62-81, Jan. 1998.

[5] B. Ma, S. Lakshmanan and A. O. Hero, "Simultaneous detection of lane and pavement boundaries using model-based multisensor fusion", *IEEE Trans. Intell. Transport. Syst.*, Vol.1, No.3, pp.135-147, Sept. 2000.

[6] M. Nikolova and A. Hero, "Segmentation of a road from a vehicle-mounted radar and accuracy of the estimation", in *Proc. of the IEEE Intel. Veh. Symp.*, Dearborn, 2000, pp. 284-289.

[7] J. Sparbert, K. Dietmayer and D. Streller, "Lane detection and street type classification using laser range images", in *Proc. IEEE ITSC*, California, 2001, pp.454-459.

[8] A. Kirchner and T. Heinrich, "Model based detection of road boundaries with a laser scanner", in *Proc. Intl. Conf. Intelligent Vehicles*, 1998, pp.93-98.

[9] S. S. Ge and Y. J. Cui, "New potential functions for mobile robot path planning", *IEEE Trans. Robot. Automat.*, Vol. 16, No. 5, pp.615 -620, Oct. 2000.

[10] S.S. Ge and Y. J. Cui, "Dynamic motion planning for mobile robots using potential field method", *Autonomous Robots*, Vol. 13, no. 3, 2002.

[11] Y. J. Cui and S.S. Ge, "Autonomous vehicle positioning with GPS in urban canyon environments", *IEEE Trans. Robot. Automat.*, Vol. 19, No. 1, pp. 15-25, 2003.

[12] W.S. Wijesoma, K.R.S. Kodagoda and A.P. Balasuriya, "Laser-camera composite sensing for road detection and tracking", *Intl. Journal of Robotics and Automation* , Vol.20, No.3, 2005, pp145-157
[13] S. Blackman and R. Popoli, *Design and Analysis of Modern Tracking Systems*, Boston, Artech House, 1999.
[14] Y. Bar-Shalom and X. R. Li, *Estimation and Tracking: Principles, Techniques, and Software*, Boston, Artech House, 1993.
[15] Y. Bar-Shalom and X. R. Li, *Multitarget-Multisenor Tracking: Principles and Techniques*, Storrs CT: YBS Publishing, 1995.
[16] D. Musicki, R. Evans and S. Stankovic, "Integrated probabilistic data association", *IEEE Trans. Automat. Contr.*, Vol. 39, No. 6, pp.1237-1241, June 1994.
[17] R. E. Helmick, and G. A. Watson, "IMM-IPDAF for track formation on maneuvering targets in cluttered environments", *Signal and Data Processing of Small Targets 1994, Proc. SPIE*, Vol. 2235, pp. 460-471, Apr. 1994.
[18] A. Houles and *Y.* Bar-Shalom, "Multisensor Tracking of a Maneuvering Target in Clutter", *IEEE Trans. Aerospace and Elect. Systems*, Vol. AES – 25, No.2, pp.176-189, March 1989.
[19] F. Dufour and M. Mariton, "Tracking a 3D maneuvering target with passive sensors", *IEEE Trans. Aero. and Elect. Sys.*, Vol. 27, Issue 4, pp. 725 – 739, July 1991.
[20] T. Kirubarajan, Y. Bar-Shalom, and E. Daeipour, "Adaptive beam pointing control of a phased array radar in the presence of ECM and false alarms using IMMPDAF", *Proc. American Control Conf.*, Vol. 4, Seattle, 1995, pp. 2616 – 2620.
[21] S. Julier, J. Uhlmann, H. F. Durrant-Whyte, "A new method for the nonlinear transformation of means and covariances in filters and estimators", *IEEE Trans. Automat. Contr.*, Vol. 45, No.3, pp.477-482, Mar. 2000.
[22] B. Chen and J. K. Tugnait, "Multisensor tracking of a maneuvering target in clutter using IMMPDA fixed-lag smoothing", *IEEE Trans. Aerospace and Electronics Syatems*, Vol. 36, No. 3 pp.983-991, July 2000.

K. R. S. Kodagoda received the B.Sc. Eng. Hons. degree in electrical engineering from the University of Moratuwa, Sri Lanka, in 1995. He received the M.Eng. and the PhD from Nanyang Technological University, Singapore in 2000 and 2004. He is currently working as a Research Fellow in the ARC Centre of Excellence for Autonomous Systems (CAS), Sydney, Australia.

He was a Design and Sales Engineer with Toroid International Pvt. Ltd. from 1996 to 1998. From 2000 to 2002, he was a Research Associate in the project "Development of an autonomous navigation system for an outdoor autonomously guided vehicle – (ARC 3/95)," with Nanyang Technological University, contributing to the design and development of the automated guided vehicle. In 2004, he was a Research Associate at National University of Singapore working on Intelligent Control of Unmanned Vehicles. His current research interests are on environment perception, intelligent transportation systems and unmanned ground vehicles.

Dr. Kodagoda is a Member of the IEE and Associate Member of the Institution of Engineers, Sri Lanka. His biography is published in *Who's Who in Science and Engineering* (New Providence, NJ: Marquis, 7th ed., 2003). He is a reviewer of the IEEE Trans. on Vehicular Technology and IEEE Trans. on SMC.

Shuzhi Sam Ge, IEEE Fellow, PEng (Singapore), is a Full Professor with the Department of Electrical and Computer Engineering, the National University of Singapore. He received his BSc degree from the Beijing University of Aeronautics and Astronautics (BUAA) in 1986, and the PhD degree and the Diploma of Imperial College (DIC) from the Imperial College of Science, Technology and Medicine in 1993. He has (co)-authored three books: Adaptive Neural Network Control of Robotic Manipulators (World Scientific, 1998), Stable adaptive Neural Network Control (Kluwer, 2001) and Switched Linear Systems: Control and Design (Springer-Verlag, 2005), over 200 international journal and conference papers, and co-invented 3 patents. He served/serves as an Associate Editor for IEEE Transactions on Automatic Control, IEEE Transactions on Control Systems Technology, Automatica, IEEE Transactions on Neural Networks, Corresponding Editor for Asia and Australia, IEEE Control Systems Magazine, and Editor of International Journal of Control, Automation, and Systems. His current research interests are in adaptive neural network control, hybrid systems, intelligent vehicles and system development.

W. Sardha Wijesoma (M'99) received the BSc. Engineering Hons. degree in electronics and telecommunication engineering from the University of Moratuwa, Sri Lanka, in 1983, and the Ph.D. degree in robotics from Cambridge University, Cambridge, U.K., in 1990. He is an Associate Professor of the School of Electrical and Electronic Engineering, Nanyang Technological University (NTU), Singapore. He is also the Program Director for Mobile Robotics of the Center for Intelligent Machines, NTU. He was previously the Head of the Department of Computer Science and Engineering, University of Moratuwa, Sri Lanka. His research interests are in autonomous land and underwater vehicles, with emphasis on problems related to navigation and perception.

Dr. Wijesoma is a member of the British Computer Society and a Chartered Information Systems Engineer (C. Eng.) of the Engineering Council of the U.K. He is a founding committee member of the IEEE Systems, Man, and Cybernetics Society Chapter, Singapore, Committee Member of IEEE Oceanic Engineering Society Chapter, Singapore and Technical Co-chair of OCEANS'06 Asia Pacific IEEE Conference, Singapore.

Arjuna Balasuriya received his B.Sc.(hons) Engineering and Master of Philosophy degrees in electrical and electronic engineering from the University of Peradeniya, Sri Lanka, in 1992 and 1994, respectively, and the Doctor of Engineering degree from the University of Tokyo, Japan, in 1998. He was a Japan Society for the Promotion of Science (JSPS) research fellow during 1998-1999 and a visiting JSPS fellow during 1999-2002 at the University of Tokyo. He was an assistant professor in the School of Electrical and Electronic Engineering, Nanyang Technological University, Singapore during 1999 - 2005.Currently he is a research scientist at the Massachusetts Institute of Technology, USA. He was the consultant on autonomous navigation for the undersea defense project Cassiopeia in Singapore. His current research interests include robotics and automation, artificial intelligence, computer vision, embedded systems, real-time systems, and underwater robotics. He has published more than 100 journal and conference papers and has co-authored two book chapters. Dr. Balasuriya is a reviewer of the International Journal of Engineering Applications in Artificial Intelligence (Elsevier Science, New York and Amsterdam), and IEEE Intelligent Systems magazine. He is the chapter chair of IEEE Oceanic Engineering Society Singapore and general co-chair for the OCEANS'06 Asia Pacific IEEE conference.